Monatshefte für Chemie 111, 1367—1390 (1980)

Monatshefte für Chemie

Small-Angle X-Ray Scattering Studies on the X-Ray Induced Aggregation of Malate Synthase I. Structural and Kinetic Studies

Peter Zipper[a, *] and **Helmut Durchschlag**[b]

[a] Institut für Physikalische Chemie, Universität Graz, A-8010 Graz, Austria

[b] Institut für Biophysik und Physikalische Biochemie, Universität Regensburg, D-8400 Regensburg, Federal Republic of Germany

(Received 29 April 1980. Accepted 10 June 1980)

Small-angle X-ray scattering measurements on malate synthase in aqueous solution revealed a continuous increase of the intensity in the innermost portion of the scattering curve with increasing measuring time. We have definite evidence that this increase reflects an X-ray induced aggregation of the enzyme particles in the course of the small-angle X-ray scattering experiment. Obviously this aggregation is a consequence of a radiation damage of the particles by the primary beam used in the scattering experiment.

The aggregation process of malate synthase was monitored *in situ* by small-angle X-ray scattering. For this purpose scattering curves were taken at various stages of aggregation. The analysis of these curves established the increase of the particle dimensions, the retention of the pseudo thickness factor of the native enzyme and the occurrence of one and later on of two pseudo cross-section factors. These results suggest the way how the aggregation might proceed. The results led to a tentative model of the aggregation process in which a one-dimensional side-by-side association of the oblate enzyme particles is followed by a two-dimensional aggregation. An aggregation in the third dimension was not observed during the time covered by our experiment.

The time dependence of molecular parameters, for instance of the apparent mean radius of gyration, was used to compare the aggregation of enzyme samples that were irradiated under different experimental conditions. The addition of dithiothreitol to the enzyme solutions as well as the presence of the substrates or of a substrate analogue or of ethanol were found to reduce the rate of aggregation.

(Keywords: Aggregation process, model; Malate synthase; Radioprotection; Small-angle X-ray scattering; Structure and kinetics; X-Ray induced aggregation)

0026-9247/80/0111/1367/$ 04.80

Röntgenkleinwinkeluntersuchungen der durch Röntgenstrahlen induzierten Aggregation der Malatsynthase. I. Strukturuntersuchungen und kinetische Messungen

Röntgenkleinwinkeluntersuchungen an wäßrigen Lösungen von Malatsynthase zeigten eine mit der Meßdauer ansteigende Zunahme der Streuintensität im Innenteil der Streukurve. Dieser Intensitätsanstieg spiegelt zweifelsohne eine durch die Röntgenbestrahlung induzierte Aggregation der Enzymteilchen während der Röntgenkleinwinkelmessung wider. Diese Aggregation ist offensichtlich auf einen durch die Primärstrahlung verursachten Strahlenschaden zurückzuführen.

Das Fortschreiten der Aggregation der Malatsynthase wurde mit Hilfe der Röntgenkleinwinkelstreuung *in situ* verfolgt. Zu diesem Zweck wurden Streukurven bei verschiedenen Aggregationsstadien aufgenommen. Die Analyse dieser Kurven zeigte die Zunahme der Teilchendimensionen, das Beibehalten des Pseudodickenfaktors des nativen Enzyms und das Auftreten eines und später zweier Pseudoquerschnittsfaktoren an. Diese Ergebnisse lieferten Hinweise, wie die Aggregation ablaufen könnte, und führten zu einem möglichen Modell für den Aggregationsvorgang. Demnach sollte auf eine eindimensionale, laterale Aggregation der oblaten Enzymteilchen eine zweidimensionale Aggregation folgen. Ein Fortschreiten der Aggregation in der dritten Dimension konnte während der Dauer des Experimentes nicht beobachtet werden.

Die zeitliche Abhängigkeit molekularer Parameter, z. B. des apparenten mittleren Streumassenradius, wurde für den Vergleich der Aggregation von Enzymproben, die unter verschiedenen experimentellen Bedingungen bestrahlt wurden, herangezogen. Durch Zugabe von Dithiothreitol oder Ethanol zu den Enzymlösungen oder durch die Anwesenheit der Substrate oder eines Substratanalogen konnte die Aggregationsgeschwindigkeit herabgesetzt werden.

Introduction

Malate synthase (EC 4.1.3.2) is a shunt-enzyme in the glyoxylic acid cycle; it catalyzes the synthesis of malate from acetyl-CoA and glyoxylate[1–4].

An electrophoretically pure enzyme has been prepared from baker's yeast[5] and has been characterized by chemical, ultracentrifugal, spectroscopic, electron microscopic and small-angle X-ray scattering (SAXS) investigations[5–12]. The yeast enzyme has a molecular weight of about 180,000 and is of oblate shape (axial ratio about 1 : 1/3). Evidence for the occurrence of structural changes upon binding of the substrates (acetyl-CoA, glyoxylate) or of the substrate analogue pyruvate was obtained from spectroscopic, hydrodynamic and SAXS studies. The enzyme has a total of 17 ± 1 sulfhydryl groups; 3.6 ± 0.2 sulfhydryl groups of the enzyme were found in the absence of denaturing agents and turned out to be essential for biological activity. The enzyme could be split into subunits by a variety of denaturants. The occurrence of a single band in electrophoretic studies in the presence of sodium dodecyl sulfate indicates dissociation of the enzyme to identical or very similar subunits. Comparison of the molecular weights for the native enzyme

and for the subunits suggested the quaternary structure of the enzyme to be trimeric rather than tetrameric. Further hints for a trimeric structure were obtained from electron micrographs which showed particles with three-fold symmetry, and also from the SAXS studies which revealed an increase of the molecular weight of the enzyme upon saturation with acetyl-CoA, corresponding to the binding of 2.7 ± 1 molecules of this substrate.

During the SAXS measurements for the structural characterization of the enzyme and of enzyme-substrate complexes[10,11], we observed the occurrence of small changes in the scattering curves, with increasing measuring time. These changes obviously reflected an aggregation of the enzyme, possibly as a consequence of radiation damages[13,10,14].

The occurrence of radiation damages of proteins upon X-irradiation in aqueous solution is a phenomenon well-known to radiobiologists[15–19]. These damages which occur mainly by the indirect effect of radiation, i.e. by the radiolysis products of water ($H^{\cdot}$, $OH^{\cdot}$, $HO_2^{\cdot}$, O_2^{-}, e_{aq}^{-}, H_2O_2), may include chain cleavage, changes in amino acid composition, destruction of secondary and tertiary structure, aggregation etc. The formation of different kinds of radicals has been established by various methods including pulse radiolysis, UV- and ESR-techniques. In the case of enzymes, enzymic activity was used as a tool for following the inactivation of damaged particles. Structural characterizations of the irradiated products have been performed till now by a variety of experimental techniques (e.g. gel filtration, ultracentrifugation, viscometry, light scattering, electrophoresis). None of these methods is able to provide such detailed information on the three-dimensional structure of dissolved particles as the SAXS technique. Therefore we applied SAXS to investigate the X-ray induced damage of malate synthase in detail.

We started this investigation mainly for two reasons: (i) to demonstrate for the first time the feasibility of SAXS in the field of radiation biology, i.e. to investigate the structure of damaged enzyme particles and the kinetics of their formation, (ii) to look for possibilities to suppress or reduce radiation damages of biopolymers in the course of conventional SAXS experiments. The latter aspect was a necessary prerequisite for the detailed SAXS investigations of the native enzyme and especially of enzyme-substrate complexes[10,11], where we had to differentiate between structural changes due to substrate binding or due to radiation effects.

The results from our studies on the X-ray damage of malate synthase will be presented in this and a following paper (Part II)[20], from the point of view of SAXS. Some radiobiological aspects of our investigations have been outlined elsewhere[24].

Materials and Methods

Materials

Dithiothreitol (*DTT*) was obtained from Calbiochem, CoA and acetyl-CoA from Boehringer, glyoxylate and pyruvate from Merck. All other reagents were of A-grade purity. Quartz-bidistilled water was used throughout. For some preliminary experiments acetyl-CoA was prepared by the method of *Simon* and *Shemin*[21].

Enzyme Solutions

Malate synthase from baker's yeast was prepared and purified as described in Ref.[11]. Stock solutions of enzyme were obtained by extensive dialysis at 4 °C against $5\,mM$ Tris-HCl buffer, $pH\,8.1$, containing $10\,mM\,MgCl_2$, $1\,mM\,MgK_2EDTA$ and 0, 0.2 or $2\,mM\,DTT$. The enzyme solutions and the dialysis buffers were stored at 4 °C. Before use, the enzyme solutions were centrifuged for 30 minutes at 15,000 rpm in a Sorvall RC2-B centrifuge. The enzyme concentrations were determined spectrophotometrically[5]; they varied from about 7 to 42 mg/ml. Solutions of the enzyme-substrate complexes were prepared by adding calculated volumes of concentrated aqueous solutions of the substrates to the enzyme solution. The final concentrations of these ligands amounted to $90\,mM$ glyoxylate, $50\,mM$ pyruvate, $2\,mM$ acetyl-CoA; this corresponds to a degree of saturation of the enzyme to about 90-99%, as may be calculated from the dissociation constants for the various enzyme-substrate complexes: $K_M = K_s = 8.3 \cdot 10^{-5}\,M$ for the substrate acetyl-CoA, $K_M = K_s = 1 \cdot 10^{-4}\,M$ for the substrate glyoxylate, $K_i = 5.4 \cdot 10^{-4}\,M$ for the substrate analogue pyruvate[22,3].

Previous ultracentrifugal experiments[8] under identical conditions of buffer and temperature, as used for the X-ray measurements, at concentrations $c > 0.1$ mg/ml have shown that no dissociation or association of the native enzyme occurs in the absence or presence of the substrates.

Small-Angle X-Ray Scattering

The X-ray source was a water-cooled tube with copper target and focus of $2 \times 12\,mm^2$ (Philips PW 2253/10) that was driven by a Philips PW 1140 power supply. The applied voltage was 50 kV, the current was either 8 or 30 mA.

SAXS experiments were performed by means of a *Kratky* camera with slit collimation[23,24], that was adjusted on the broad side of the focus. The width of the entrance slit was 150 μm. The samples were investigated in *Mark* capillaries at 4 °C; they were irradiated by the collimated, but nearly unfiltered radiation. A proportional counter tube in connection with a pulse height discriminator set to receive the CuK_α-line ($\lambda = 0.154$ nm) was used to record the scattered radiation. The amount of CuK_β-radiation ($\lambda = 0.139$ nm) was determined as described elsewhere[25]. The integral intensity P_0 of the primary beam was determined by means of a calibrated lupolen platelet as secondary standard[26].

Measurements of X-ray scattering were performed in an angular range from about 3 to 125 mrad. For many experiments, however, the angular range was reduced by omitting measurements at large angles. The curves were scanned stepwise whereby for each measuring point usually 40,000 pulses were counted. Each scattering curve was measured repeatedly; this was facilitated by means of a programmable step scanning device that allowed a fully automatic operation[27]. For all samples, the blank curves, originating from the scattering

of the solvent and the capillary, were determined in the same way as the scattering from the solutions. Averaging over repeatedly measured blank curves yielded a mean blank curve, which was subtracted from the respective solution scattering curves as obtained from a series of subsequent goniometer runs. Thus each solution scattering curve was evaluated separately. The difference curves were then corrected for collimation effects and for the influence of the Cu K_β-line that was not suppressed by the pulse height discriminator. An extrapolation to zero concentration could not be performed for reasons discussed later on. A series of computer programs developed in the Institute of Physical Chemistry, University of Graz, facilitated the performance of the above operations[28–30]. Calculations were performed on a UNIVAC 494 and on an IBM 1130 computer.

Theory

The theory of SAXS has been described in detail[31–35]. Here we will only present briefly some relations necessary for better understanding.

The intensity I_0 scattered at zero angle and the radius of gyration R were determined from logarithmic plots of the desmeared scattering curves according to *Guinier*'s exponential law, or from the distance distribution functions $p(r)$ obtained by *Fourier* inversion of the desmeared scattering curves. The molar mass M was determined from the absolute value I_0/P_0 of the zero intensity. The apparent quantities $\bar{I}_0$ and $\bar{R}$ were determined from the slit-smeared scattering curves. The cross-sectional radius of gyration R_c and the thickness radius of gyration R_t were derived from cross-section or thickness *Guinier* plots of the desmeared scattering curves.

In the case of polydisperse solutions the parameters obtained represent mean values, e.g.

$$\bar{I}_0 = \sum w_i I_{0i} \tag{1}$$

$$\bar{M} = \sum w_i M_i \tag{2}$$

$$\bar{R}^2 = \frac{\sum w_i I_{0i} R_i^2}{\bar{I}_0} = \frac{\sum w_i M_i R_i^2}{\bar{M}}, \tag{3}$$

where w_i is the weight fraction of species i. According to the above definitions, $\bar{I}_0$ and $\bar{M}$ are weight-averages and $\bar{R}^2$ is a z-average. Thus the mean radius of gyration $\bar{R}$ itself is the square-root of a z-average. The mean degree of aggregation, $\bar{x}$, as obtained by dividing $\bar{I}_0$ from a solution of aggregates by I_0 from a solution of monomers of the same concentration, is also a weight-average. The mean squares of R_c and of R_t are defined by relations similar to eq. (3).

If a particle is an aggregate of N identical monomers of radius of gyration R_1, the radius of gyration of this aggregate is given by

$$R^2 = R_1^2 + \frac{\sum_N l_i^2}{N}, \tag{4}$$

where l_i is the distance of the centre of gravity of the i-th monomer from the centre of gravity of the entire aggregate.

Results and Discussion

1. Evidence for X-Ray Induced Aggregation

The scattering behaviour of malate synthase changed significantly during prolonged X-irradiation. Subsequently measured SAXS curves revealed a steady increase of intensity in the innermost portion (Fig. 1).

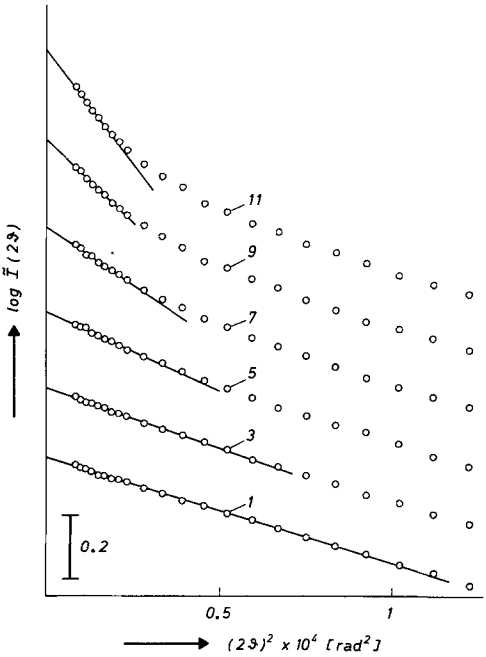

Fig. 1. *Guinier* plots of selected experimental slit-smeared scattering curves of aggregating malate synthase ($c = 26.6$ mg/ml, 0.2 *mM DTT*). The time interval between two subsequent curves is 11.4 hours. The vertical position of the curves is arbitrary

These changes correspond to an increase of both the molecular weight and the radius of gyration and obviously reflect an aggregation process.

Since enzyme that was not exposed to X-rays is rather stable and can be stored at 4 °C for several weeks without any significant change of the initial scattering behaviour, the aggregation observed during the scattering experiments must be assumed to be X-ray induced. This was further corroborated by the following experiments.

A sample of malate synthase was investigated in the small-angle camera for 27.5 hours and during this time 22 scattering curves were recorded. Analysis of the experimental curves showed, that during the

experiment the apparent mean radius of gyration $\tilde{R}_u$ of the enzyme had increased by a factor of 2.08. Another sample from the same enzyme solution was in the camera for a total of 39 hours under conditions very similar to those in the first experiment, except that now the X-irradiation was interrupted two times for several hours. Thus the sample was actually irradiated for a time practically identical to that for the first sample. The apparent mean radius of gyration $\tilde{R}_i$ of the enzyme at the end of the experiment was found to be larger by a factor of 2.16 than the initial value.

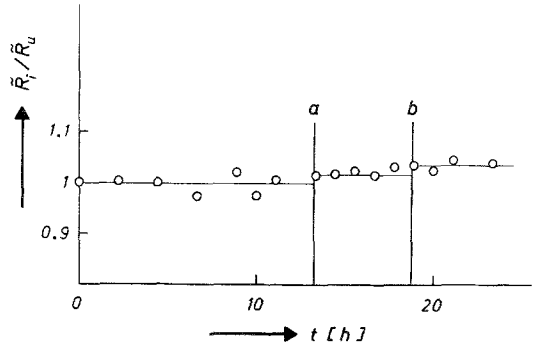

Fig. 2. Plot of the quotient $\tilde{R}_i/\tilde{R}_u$ for two samples of malate synthase ($c = 16.0$ mg/ml, 0.2 mM DTT) versus the time t of X-irradation. $\tilde{R}_u$: apparent mean radius of gyration of uninterruptedly irradiated enzyme; $\tilde{R}_i$: apparent mean radius of gyration of enzyme, the irradiation of which was interrupted for 8.4 hours (a) and 3.3 hours (b)

In Fig. 2, the ratio of the apparent mean radii of gyration, $\tilde{R}_i/\tilde{R}_u$, of the two samples is plotted versus the time of irradiation. Breaks in the irradiation of the second sample are marked by vertical lines. As can be seen, $\tilde{R}_i/\tilde{R}_u$ is approximately equal to unity over the entire time range, with only slight increases ($<4\%$) that obviously occurred during the interrupts of irradiation. This figure clearly shows, that the aggregation process (as it is reflected by the increase of $\tilde{R}_u$ and $\tilde{R}_i$ by more than 100% during the experiment) is essentially X-ray dependent and comes almost to a standstill when the X-irradiation is stopped. Nevertheless, the small increases of $\tilde{R}_i/\tilde{R}_u$ at the breakpoints in Fig. 2 suggest that an aggregation takes place even without stimulating irradiation at a, however, much lower rate. Additional evidence for the occurrence of such a slow aggregation of a previously irradiated enzyme was obtained from the observation that $\tilde{R}$ of a sample further increased within 10 days after irradiation from the 1.6 fold to the 2.6 fold of the initial value for the native enzyme.

It is very probable that both the aggregation observed during the X-irradiation of the enzyme solutions and the slower aggregation occurring after the irradiation have a common origin, namely damages of enzyme particles caused by radiation. Since the enzyme is in aqueous solution, it can be expected that most of the primary radiation damages occur through the so-called indirect effect of radiation.

Surely, not every damage occurring in this way will immediately lead to the formation of aggregates of enzyme particles. However, as long as the enzyme solution is irradiated, the steady production of radiolysis products of water will maintain the steady occurrence of radiation damages and the formation of aggregates. After the irradiation has been stopped and the primary radicals and other radiolysis products have been used up, those radiation damages of enzyme particles, that had not caused aggregation immediately, may give rise to the formation of further aggregates in a much slower process.

Extensive X-irradiation of enzyme samples led to a macroscopic turbidity of the solution, and finally to a gel-like state.

2. Structural Studies

Slit-Smeared Scattering Curves

Fig. 1 shows *Guinier* plots of the innermost portions of experimental slit-smeared scattering curves as obtained from every second run of a typical series of measurements on the enzyme. A summary of results derived from these measurements is given in Table 1.

Curve 1 of Fig. 1 was taken immediately after the fresh enzyme solution was filled into the capillary. The measurement of the innermost portion of the curve as shown in the figure was completed in about half an hour, while the measurement of the rest of the curve (not shown in the figure) took a much longer time. The time interval (irradiation time only) between two subsequent runs was 5.7 hours. As can be seen from Table 1, the increase of $\tilde{R}$ from the first to the second run amounts to only 0.1 nm. This implies that the change of $\tilde{R}$ during the measurement of the innermost portion of the first scattering curve did not exceed about 0.25%. The increase of $\tilde{I}_0$ must have been even considerably lower. This fully justifies to consider curve 1 as representative for the native unaggregated enzyme. However, even at the most advanced stages of aggregation (runs 9–11, cf. Table 1), the changes of $\tilde{R}$ within the time needed to measure the innermost portions of the scattering curves are below 1% while the changes of $\tilde{I}_0$ do not exceed 2.5%. Thus also the innermost portions of the scattering curves of the highly aggregated enzyme can be considered in good approximation as

snapshots of the enzyme sample taken after well-defined times of irradiation.

As a consequence of the aggregation process the initial homodispersity of the enzyme solution has gone lost after some time. Therefore the scattering curves contain information simultaneously on both unaggregated and different species of aggregated enzyme particles. All parameters derived from these scattering curves therefore represent mean values.

Two further points must be considered. The measurements were performed at an enzyme concentration ($c = 26.6$ mg/ml) where interparticular interferences usually cause a noticeable reduction of the intensity in the innermost portion of the scattering curve. An elimination of the interferences in the conventional way by extrapolation to zero concentration (after measurements at various different enzyme concentrations) appeared to be useless because of a possible influence of the enzyme concentration on the aggregation process. The amount of the intensity decrease due to interferences is only known for the unaggregated enzyme (cf. Ref.[11]). Here, at the same high enzyme concentration, the interferences led to a decrease of $\tilde{R}$ by 6% and to a decrease of $\tilde{I}_0$ by 11%, as compared to the corresponding values at zero concentration. No predictions can be made on the size of interference effects for the aggregated enzyme. However, it will be useful to assume in first approximation, that they are of similar relative size as for the unaggregated enzyme. In this case, the relative changes of parameters (e.g. of $\tilde{R}$ and $\tilde{I}_0$) would be obtained correctly even though the parameters themselves are affected by the interferences.

The second point that must be considered concerns the possible influence of the limitation of the scattering curves towards the smallest angles as caused by the resolution of the collimation system. It cannot be excluded completely that at the most advanced stages of aggregation (cf. curves 9 and 11 in Fig. 1) the resolution was insufficient. This means, that possibly in the *Guinier* plots of the corresponding scattering curves a further increase of intensity towards zero angle above the plotted straight lines would have shown up if the measurements would have been extended down to smaller angles. (This was, however, impossible with the entrance slit width used.) Thus the observed increase of $\tilde{R}$ and of $\tilde{I}_0$ by about 100% upon irradiation of the enzyme for 57.2 hours is possibly underestimated.

Desmeared Scattering Curves

Correction of the experimental scattering curves for collimation and wavelength effects yielded desmeared curves some of which are shown in a semi-logarithmic plot in Fig. 3. The most pronounced changes of

scattering behaviour due to aggregation obviously occur in the innermost portion of the scattering curves, while at medium scattering angles the curves are very similar to each other. Further differences at large angles are probably due to experimental and numerical errors involved by the low pulse rate and the desmearing procedure.

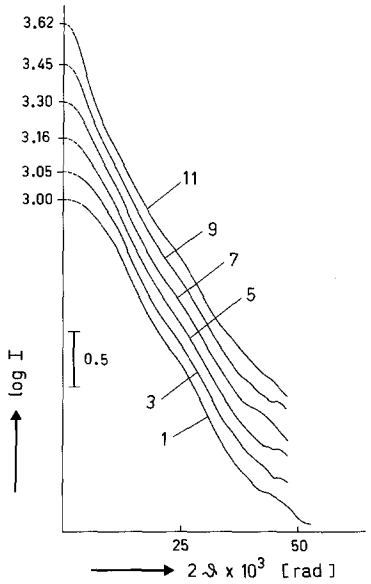

Fig. 3. Selected desmeared scattering curves of aggregating malate synthase ($c = 26.6$ mg/ml, 0.2 *mM DTT*). The time interval between two subsequent curves is 11.4 hours. The vertical position of the curves is arbitrary

Guinier plots of the desmeared curves similar to those shown in Fig. 1 yielded the mean radii of gyration (designated $\bar{R}_G$) listed in Table 1. As compared to the values of $\tilde{R}$ determined directly from the slit-smeared curves, the values obtained for $\bar{R}_G$ are generally larger, the differences ranging from about 1.5% at the beginning to nearly 20% at the more advanced stages of aggregation. This behaviour is easily understood, as with proceeding aggregation the angular range where the scattering curve obeys a *Gauss*ian becomes increasingly narrower* (cf. Fig. 1). The total increase of $\bar{R}_G$ during the experiment amounts to a factor of 2.41.

* $\tilde{R}$ can be considered to be a good approximation to $\bar{R}_G$ only if the *Guinier* approximation is valid over a wide angular range (cf. Ref.[36]).

Instead of the mean zero intensities $\bar{I}_0$, as derived from the *Guinier* plots of the desmeared scattering curves, we have given in Table 1 the mean degrees of aggregation $\bar{x}_G$. According to the data given in Table 1, $\bar{x}_G$ increases during the experiment from unity to 4.12, while the apparent mean degree of aggregation $\tilde{x}$ (as derived from the listed values for $\tilde{I}_0$) increases only to 1.91. The reason for this discrepancy is again found in the deviation of the scattering curves from *Gauss*ian shape with proceeding aggregation.

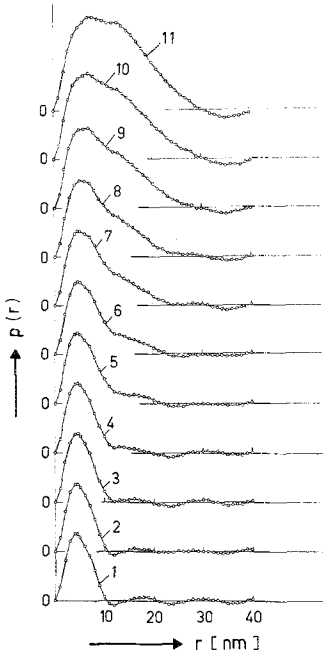

Fig. 4. Distance distribution functions $p(r)$ of aggregating malate synthase ($c = 26.6$ mg/ml, 0.2 *mM DTT*). The time interval between two subsequent curves is 5.7 hours

Distance Distribution Functions

The distance distribution functions $p(r)$ are shown for all eleven runs of the experiment in Fig. 4. Though also the $p(r)$ functions represent averages over unaggregated and aggregated enzyme particles, the curves demonstrate very convincingly the progress of aggregation.

Curve 1 of Fig. 4 goes through zero for the first time (apart from the zero at $r = 0$) at a distance r of about 10 nm, and curve 2 behaves in a similar manner. However, already curve 3 has its first zero at a distance r of about 20 nm. Beginning with curve 7 and more pronounced in

curves 8 to 11, the first zero is found to be shifted up to a distance of about 30 nm. It is interesting to note, that an inflection occurs in all curves for the later stages of aggregation at about the same radial distance as for the first zero in curve 1 (i.e. at 10 nm); a second slight inflection occurs between 20 and 30 nm.

To obtain the curves shown in Fig. 4 it was necessary to extrapolate the scattering curves beyond the experimentally accessible region to zero angle. Errors in this procedure, arising from ambiguities in approximating the *Guinier* region as well as the neglection of the effects of interparticular interferences, are mainly responsible for the oscillations of the distance distribution functions around the base-line in curves 1-8 and for the relatively deep minimum in the tail-end of curves 9-11 (cf. Ref.[37]).

The position of the first zero in curve 1 of Fig. 4 corresponds well with the diameter of the native unaggregated enzyme particle which was determined previously as 11.2 nm[11]. The positions of the zeros in the other curves represent the respective maximum visible diameters of aggregated enzyme particles. The maximum visible diameter is not necessarily identical with the maximum diameter of the largest aggregates, but it may be smaller than that diameter. This is a consequence of the oscillations of the distance distribution functions.

Quantitative evaluation of the $p(r)$ functions yielded the mean radii of gyration $\bar{R}_p$ and the mean degrees of aggregation $\bar{x}_p$ which are also listed in Table 1. It can be seen that, apart from the first two runs, the parameters $\bar{R}_p$ and $\bar{x}_p$ are generally somewhat larger than the corresponding parameters $\bar{R}_G$ and $\bar{x}_G$ as derived directly from the desmeared scattering curves. This slight discrepancy is probably due to the ambiguities in approximating the *Guinier* region in the scattering curves and to the neglection of interparticular interferences. $\bar{R}_p$ and $\bar{x}_p$ are usually less sensitive to errors in the scattering curves at smallest angles than $\bar{R}_G$ and $\bar{x}_G$ (cf. Ref.[38]).

Thickness *Guinier* Plots

Thickness *Guinier* plots of scattering curves of aggregating malate synthase (cf. Fig. 3) are shown in Fig. 5. The great similarity of all curves is obvious. The pseudo thickness factors show all the same slight oscillations around a straight line. However the slope of the line changes a little with proceeding aggregation. Thus the radius of gyration of the thickness decreases from $R_t = 1.025$ nm for the unaggreated enzyme to $\bar{R}_t = 0.925$ nm for the enzyme at the most advanced stage of aggregation.

We conclude from the retention of the original pseudo thickness factor of malate synthase (cf. Ref.[11]) during the X-ray induced

aggregation that the aggregates are also disk-like similar to the native enzyme. Our experimental findings do not indicate an increase of the thickness during aggregation. This suggests that the aggregation does not proceed in all three dimensions of the enzyme particle.

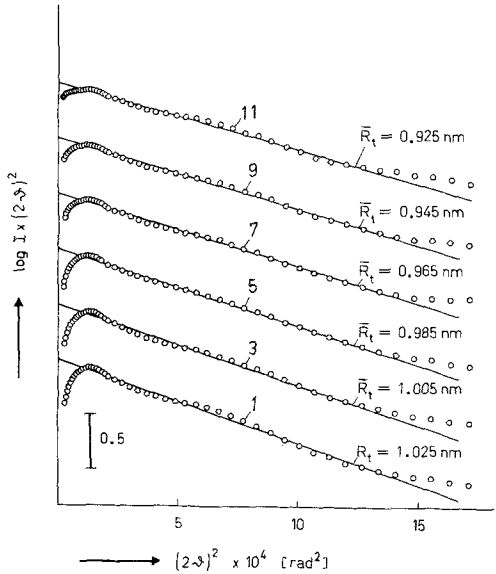

Fig. 5. Thickness *Guinier* plots of selected desmeared scattering curves of aggregating malate synthase ($c = 26.6$ mg/ml, 0.2 *mM DTT*). $\bar{R}_t$: mean radius of gyration of the thickness. The time interval between two subsequent curves is 11.4 hours. The vertical position of the curves is arbitrary

Cross-Section *Guinier* Plots

By cross-section *Guinier* plots of the scattering curves we tried to decide whether the aggregation proceeds in one or two dimensions (Fig. 6). The presence of elongate particles would be reflected by an extended linear course in such a plot. As can be seen from Fig. 6, the curves for the unaggregated enzyme and for the early stages of aggregation are approximately linear only in a very narrow range and bend downwards from the straight line towards zero angle. From the slope of the line through the data for the unaggregated enzyme we may formally calculate $R_c = 2.73$ nm. With proceeding aggregation, however, the deviation from the linear course becomes smaller. In curve 8 the majority of data points lie almost perfectly on a straight line; the slope of this line corresponds to $\bar{R}_c = 2.40$ nm. Obviously at this stage of aggregation elongate aggregates predominate.

In curves 9-11 of Fig. 6 the intensity has risen towards zero angle above the straight line. Probably this behaviour is due to the presence of aggregates with a larger cross-section than e.g. for curve 8. Therefore we have approximated this region in the curves by another straight line, from the slope of which $\bar{R}_{c1}$ can be calculated. It is of course larger

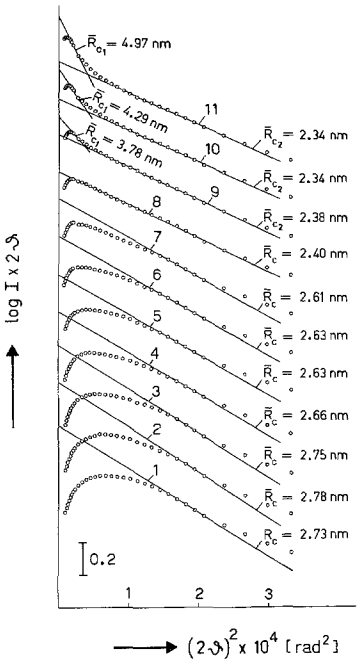

Fig. 6. Cross-section *Guinier* plots of the desmeared scattering curves of aggregating malate synthase ($c = 26.6$ mg/ml, 0.2 *mM DTT*). $\bar{R}_c$: mean radius of gyration of the cross-section. The time interval between two subsequent curves is 5.7 hours. The vertical position of the curves is arbitrary

than $\bar{R}_{c2}$ which is determined from the slope of the line through the data points at larger angles. Moreover, with proceeding aggregation $\bar{R}_{c1}$ is found to increase while $\bar{R}_{c2}$ decreases slightly.

Interpretation of Experimental Parameters

To understand the meaning of the aforementioned experimental findings, we may consider that by the following relations

$$R_c^2 = R^2 - R_t^2 \tag{5}$$

and

$$R_c^2 = (R^2 + R_t^2)/2 \tag{6}$$

Table 1. *Mean radius of gyration, mean zero intensity and mean degree of aggregation of malate synthase as a function of the time t of X-irradiation*

Run	t (h)	$\tilde{R}$ (nm)[a]	$\tilde{I}_0$[a]	$\bar{R}_G$ (nm)[b]	$\bar{x}_G$[b]	$\bar{R}_p$ (nm)[c]	$\bar{x}_p$[c]	$\bar{\bar{R}}$ (nm)[d]	$\bar{\bar{x}}$[e]
1	0	3.69_5	214	3.76	1.0	3.74_5	1.0	3.75 $\pm$ 0.01	1.0
2	5.7	3.79_5	216	3.85_5	1.02_5	3.80	1.02	3.82_5 $\pm$ 0.03	1.02
3	11.4	3.96	224	4.12_5	1.12	4.49	1.13_5	4.31 $\pm$ 0.19	1.13 $\pm$ 0.01
4	17.2	4.13_5	231.5	4.41	1.21_5	4.80	1.23_5	4.60 $\pm$ 0.2	1.22_5 $\pm$ 0.01
5	22.9	4.65	245.5	5.19_5	1.43	5.75	1.45_5	5.47 $\pm$ 0.28	1.44_5 $\pm$ 0.015
6	28.6	4.97	262.5	5.73	1.65_5	6.29	1.69	6.01 $\pm$ 0.28	1.67 $\pm$ 0.02
7	34.3	5.51	285	6.46	1.99	7.03	2.02	6.74 $\pm$ 0.29	2.01 $\pm$ 0.02
8	40.1	5.90	304	7.02	2.30	7.61	2.34	7.31 $\pm$ 0.3	2.32 $\pm$ 0.02
9	45.8	6.59	339	7.78	2.83	8.39	2.89	8.08 $\pm$ 0.31	2.86 $\pm$ 0.03
10	51.5	7.13	368	8.55	3.44	9.23	3.53	8.89 $\pm$ 0.34	3.48 $\pm$ 0.04
11	57.2	7.73	408	9.08	4.12	9.68	4.22	9.38 $\pm$ 0.3	4.17 $\pm$ 0.05

[a] Apparent mean radius of gyration $\tilde{R}$ and apparent mean zero intensity $\tilde{I}_0$, determined from the slit-smeared scattering curve.
[b] Mean radius of gyration $\bar{R}_G$ and mean degree of aggregation $\bar{x}_G$, determined from the desmeared scattering curve.
[c] Mean radius of gyration $\bar{R}_p$ and mean degree of aggregation $\bar{x}_p$, determined from the distance distribution function.
[d] Average over $\bar{R}_G$ and $\bar{R}_P$.
[e] Average over $\bar{x}_G$ and $\bar{x}_p$.

two different cross-sectional radii of gyration of the enzyme particle can be defined. Eq. (5) defines R_c around the rotational axis of the enzyme particle; with the average value for the overall radius of gyration of the unaggregated enzyme as given in Table 1 and the value for R_t as given in Fig. 6, eq. (5) leads to $R_c = 3.6\,\text{nm}$. Eq. (6) defines R_c around an axis perpendicular to the rotational axis; its value can be calculated as $R_c = 2.75\,\text{nm}$.

For geometrical reasons the value of R_c as defined by eq. (5) would also hold for linear aggregates consisting of enzyme particles which are associated along their rotational axis, while the value of R_c as defined by eq. (6) would hold for linear aggregates in which the enzyme particles are associated side-by-side.

Comparison of the above theoretical R_c values with the experimentally determined values shows, that the values found for $\bar{R}_c$ and $\bar{R}_{c2}$ favour the assumption of a one-dimensional side-by-side association of enzyme particles and rule out an association along the rotational axis. On the other hand, a strict one-dimensional association, regardless whether this aggregation occurs side-by-side or along the rotational axis, cannot account for the high value of $\bar{R}_{c1} = 4.97\,\text{nm}$ as obtained for the most aggregated enzyme sample. This result suggests that the one-dimensional aggregation must be followed by a two-dimensional aggregation. Only a two-dimensional side-by-side association can lead to aggregates with $R_c \geq 5\,\text{nm}$. The disk-like shape of such aggregates would be in accord with the experimentally found retention of the pseudo thickness factor.

As was shown above, the analysis of the scattering curves of aggregating malate synthase enabled the establishment of a tentative model of the aggregation process[14], in which a one-dimensional aggregation leading to a row of side-by-side associated enzyme particles is followed by a two-dimensional aggregation, while an aggregation in the third dimension does not occur during the time covered by our experiment.

It will be demonstrated elsewhere[37] by means of computer simulations that this model is actually consistent with most of the characteristic features of the experimentally observed scattering behaviour of aggregating malate synthase. Moreover, by calculation of theoretical curves for alternative models it will be shown, that those models represent a much poorer approximation to the aggregation process. At the moment the model outlined above is the best explanation for the results of the SAXS measurements on aggregating malate synthase.

3. Kinetic Studies

The Time Dependence of Molecular Parameters

The monitoring of aggregating malate synthase by SAXS allows statements on the kinetics of the aggregation process. The time dependence of several molecular parameters can be used to register the

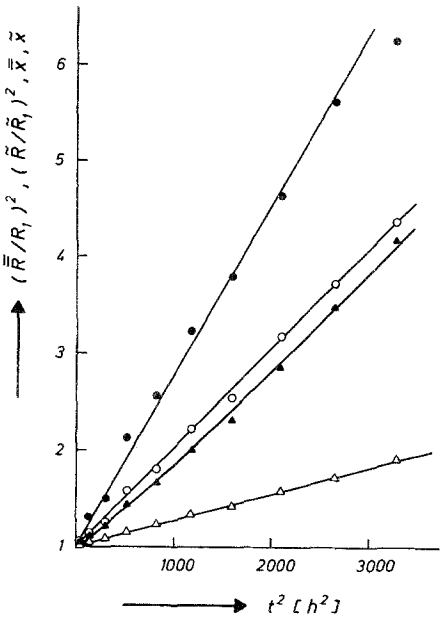

Fig. 7. Plot of the mean degree of aggregation $\bar{\bar{x}}$ (▲), of the ratio $(\bar{\bar{R}}/R_1)^2$ (●), and of the apparent parameters $\tilde{x}$ (Δ) and $(\tilde{R}/\tilde{R}_1)^2$ (○) of aggregating malate synthase ($c = 26.6$ mg/ml, 0.2 *mM DTT*) versus the square of the time t of irradiation

progress of aggregation. In Fig. 7, the average values of $\bar{\bar{x}}$ (cf. Table 1) and $(\bar{\bar{R}}/R_1)^2$ (where R_1 is the radius of gyration of the unaggregated enzyme) as well as the corresponding apparent quantities $\tilde{x}$ and $(\tilde{R}/\tilde{R}_1)^2$ are plotted versus the square of the time t of irradiation. As can be seen, both $\tilde{x}$ and $(\tilde{R}/\tilde{R}_1)^2$ depend linearly on t^2. Also the data for $(\bar{\bar{R}}/R_1)^2$ can be approximated fairly well by a straight line. On the other hand, the linear approximation of the data for $\bar{\bar{x}}$ by a straight line would give a poorer fit; these data may better be approximated by a curve reflecting a somewhat higher than quadratic dependence of $\bar{\bar{x}}$ on the time of irradiation. However, the deviation is so small that we can state, that in

first approximation all four parameters increase with the second power of the time of irradiation according to

$$A = 1 + k^2 t^2, \tag{7}$$

where A stands for any of the parameters $\bar{\bar{x}}$, $\tilde{x}$, $(\bar{\bar{R}}/R_1)^2$, $(\tilde{R}/\tilde{R}_1)^2$, and k is a rate constant. According to *Oster*[39] the intensity of light scattered from a polymerizing system should be proportional to $(1 + kt)$ if the polymerization proceeds by condensation, and proportional to $(1 + 3\,kt + k^2t^2)$ in the case of addition polymerization.

While the time dependence of $\bar{\bar{x}}$ is a direct measure for the rate of aggregation, because it reflects the changes of weight fractions of the various species of particles, the time dependence of $(\bar{\bar{R}}/R_1)^2$ reflects structural changes too. Thus not only the increase of the particle dimensions, as caused by the aggregation, but also all structural changes other than aggregation would influence this parameter. The time dependence of $(\bar{\bar{R}}/R_1)^2$ can therefore be used to characterize the velocity of structural changes caused by radiation damage.

In order to avoid the desmearing procedure, we have used the time dependence of the apparent parameter $(\tilde{R}/\tilde{R}_1)^2$ for comparing enzyme samples irradiated under different experimental conditions. We will call a plot of $(\tilde{R}/\tilde{R}_1)^2$ vs. t^2 a stability plot.

The Substrate-Free Enzyme

Stability plots for samples of substrate-free enzyme that were irradiated under various experimental conditions are shown in Fig. 8. The experimental conditions differed with respect to the concentration of enzyme, the concentration of *DTT* and the dose rate absorbed by the enzyme sample. The latter quantity can be assumed to be proportional to the integral primary intensity P_0 (expressed in CuK_α pulses per second and cm of primary beam length) for X-ray scattering. For relative measurements, the constant of this proportion need not be known as long as the absorptivity of the enzyme sample and the spectral distribution of the X-ray beam are kept constant. Unfortunately, the latter condition was not completely fulfilled in our case for technical reasons. (We had to perform the measurements by using two X-ray tubes of considerably different age and therefore of different spectral distribution.)

As can be seen from the stability plots in Fig. 8, the data for the various samples can be fitted well by straight lines, though the intercepts on the ordinate do not always equal unity. There is a strong dependence of the slope of the lines on both the primary intensity and the concentration of *DTT*. The slopes increase with P_0 and decrease upon raising the concentration of *DTT*. This can be seen even more

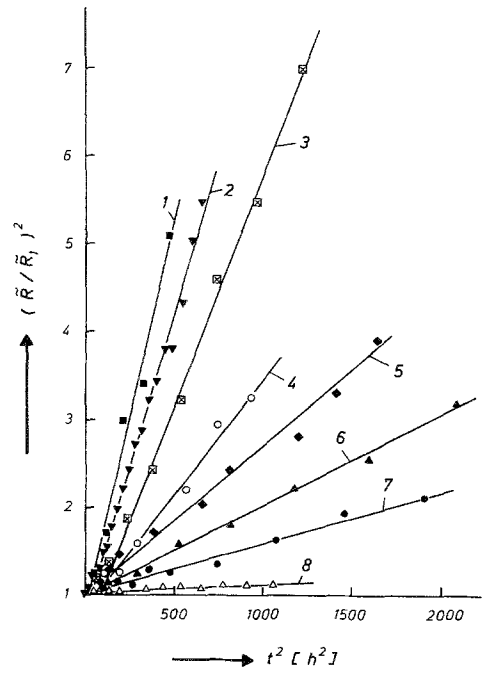

Fig. 8. Plots of the apparent parameters $(\tilde{R}/\tilde{R}_1)^2$ versus the square of the time t of irradiation for malate synthase measured under different experimental conditions. 1 (■): $c = 16$ mg/ml, integral primary intensity $P_0 = 7.89 \cdot 10^7$ counts $s^{-1}\,cm^{-1}$; 2(▼): $c = 16$ mg/ml, $P_0 = 7.48 \cdot 10^7$ counts $s^{-1}\,cm^{-1}$; 3 (⊠): $c = 7.8$ mg/ml, $P_0 = 7.11 \cdot 10^7$ counts $s^{-1}\,cm^{-1}$; 4 (○): $c = 15.4$ mg/ml, $P_0 = 8.57 \cdot 10^7$ counts $s^{-1}\,cm^{-1}$; 5 (◆): $c = 41.7$ mg/ml, $P_0 = 4.31 \cdot 10^7$ counts $s^{-1}\,cm^{-1}$; 6 (▲): $c = 26.6$ mg/ml, $P_0 = 3.84 \cdot 10^7$ counts $s^{-1}\,cm^{-1}$; 7 (●): $c = 16$ mg/ml, $P_0 = 2.12 \cdot 10^7$ counts $s^{-1}\,cm^{-1}$; 8 (Δ): $c = 21.8$ mg/ml, $P_0 = 2.12 \cdot 10^7$ counts $s^{-1}\,cm^{-1}$. Closed symbols refer to 0.2 *mM DTT*, open symbols to 2 *mM DTT*. Sample 3 (⊠) contained no *DTT*

convincingly in Fig. 9, where the logarithms of the slopes k_R^2 of the straight lines from Fig. 8 are plotted versus P_0. According to this picture, there are two distinct groups of data, namely for low and for high concentrations of *DTT*, respectively. We have fitted the data in this plot by two straight lines of similar slope. However, in doing so we have neglected a possible dependence of the results on the enzyme concentration and also the above mentioned use of two different X-ray tubes. With these restrictions, Fig. 9 suggests an exponential dependence of k_R^2 on the intensity of the X-ray beam.

On the other hand, our results for low concentration of *DTT* include data, that were obtained from the same enzyme preparation and were

measured at the same enzyme concentration (16 mg/ml) by using the same X-ray tube; thus negative influences of enzyme concentration or changes of spectral distribution of the primary radiation can be excluded in this case. Analysis of these data shows that they stand also in very good agreement with a variation of $k_{\tilde{R}}^2$ with the square of the primary intensity.

At the moment, we have not enough data to make a final decision in favour of a definite relation between $k_{\tilde{R}}^2$ and the intensity of the X-ray beam (or the absorbed dose rate). However we find it useful, to consider

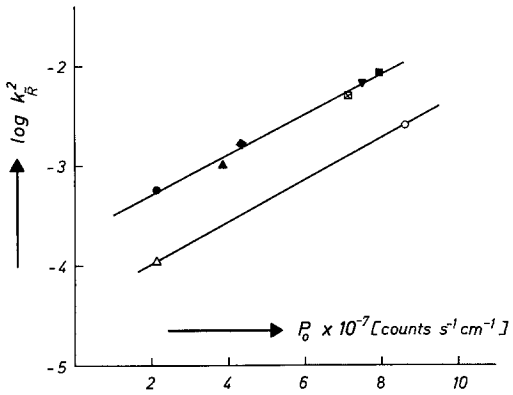

Fig. 9. Plot of log $k_{\tilde{R}}^2$ versus the integral primary intensity P_0. $k_{\tilde{R}}^2$ is the slope of any of the straight lines through the data in Fig. 8. The meaning of the symbols is the same as in that figure

some practical consequences of the two different relations mentioned above. According to eq. (7), the time t_2 at which $\tilde{R}^2$ has increased to the two-fold of its original value, is given by $1/k_{\tilde{R}}$. The product of t_2 multiplied by P_0 is proportional to the X-ray dose D_2 that must be absorbed by the enzyme sample in order to produce an increase of $\tilde{R}^2$ by 100%. A dependence of $k_{\tilde{R}}^2$ on the square of the primary intensity would then imply, that D_2 is a constant, independently from the applied dose rate.

On the other hand, an exponential dependence of $k_{\tilde{R}}^2$ on the primary intensity as suggested by Fig. 9 would imply, that D_2 varies with the dose rate and is smaller for a high dose rate than for a lower dose rate. This may have consequences for the practice of X-ray scattering. Namely to keep radiation damage of the enzyme during an X-ray experiment low, it would be better in this case to use a low instead of a high primary intensity. However this advantage of low primary

intensity could be compensated by an initial lag of aggregation as it is possibly indicated for the high intensity data in Fig. 8 by the deviation of the intercepts of the straight lines from unity. On the other hand, the mere movement of the detector along the entire angular range of a scattering curve takes also a certain time (one hour or more) during which the enzyme sample is permanently irradiated. This time is an apparative constant which is independent of the primary intensity. It is evident, that this time will play a lesser role when the radiation damage of the sample occurs slowly, due to the application of a low dose rate, than when the sample is irradiated with a high dose rate and radiation damage occurs correspondingly faster. This argument would hold true also when k_R^2 varies with the second power of the dose rate. Therefore the SAXS studies on the structure of the native substrate-free malate synthase and the enzyme-substrate complexes were performed preferably by using low primary intensities (cf. Ref.[11]).

Enzyme-Substrate Complexes

Fig. 10 shows stability plots for various enzyme-substrate complexes prepared from the same enzyme sample and investigated under almost identical experimental conditions with respect to enzyme concentration and primary intensity. For better comparison we have included in the figure also the corresponding curve for the unliganded enzyme at the same concentration of *DTT* (0.2 *mM*) and a second curve for the unliganded enzyme as obtained after addition of a freshly prepared solution of *DTT* to a final concentration of 1.74 *mM*.

The presence of the substrates glyoxylate or acetyl-CoA or of the substrate analogue pyruvate leads also to a considerable decrease of the rate of aggregation. According to Fig. 10, glyoxylate is the least effective inhibitor of aggregation; acetyl-CoA seems to be more effective; the substrate analogue pyruvate, on the other hand, turns out to be a very powerful inhibitor of aggregation, comparable in its effectiveness to 1.74 *mM DTT*.

It can be stated furthermore, that the inhibition of aggregation by 1.74 *mM DTT* is in this case considerably more effective than by the 2 *mM* solutions used for the former experiments the results of which are shown in Figs. 8 and 9. A reason for this discrepancy might be the fact that the enzyme samples for the former experiments had been stored in the presence of 2 *mM DTT*, while in the above case a freshly prepared solution of *DTT* was added to the enzyme.

As shown by Fig. 11, addition of ethanol (cf. Ref.[40]) to the enzyme solution turned out to be slightly effective too.

A detailed discussion on the radioprotective action of *DTT* and the substrates or the substrate analogue and of ethanol will be given in

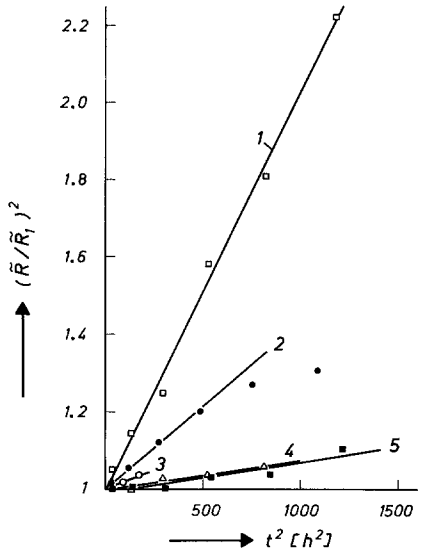

Fig. 10. Plots of the apparent parameters $(\tilde{R}/\tilde{R}_1)^2$ versus the square of the time t of irradiation for unliganded malate synthase and various enzyme-substrate complexes. **1** (□): unliganded enzyme, $c = 26.6$ mg/ml, $P_0 = 3.84 \cdot 10^7$ counts $s^{-1}\,cm^{-1}$; 2 (●): [enzyme. glyoxylate], $c = 24.2$ mg/ml, $P_0 = 3.82 \cdot 10^7$ counts $s^{-1}\,cm^{-1}$; 3 (○): [enzyme. acetyl-CoA], $c = 25.4$ mg/ml, $P_0 = 3.89 \cdot 10^7$ counts $s^{-1}\,cm^{-1}$; 4 (Δ): [enzyme. pyruvate], $c = 25.4$ mg/ml, $P_0 = 3.88 \cdot 10^7$ counts $s^{-1}\,cm^{-1}$; 5 (■): unliganded enzyme, $c = 24.2$ mg/ml, $P_0 = 3.86 \cdot 10^7$ counts $s^{-1}\,cm^{-1}$. The concentration of *DTT* was 1.74 *mM* for sample 5 and 0.2 *mM* for samples 1–4

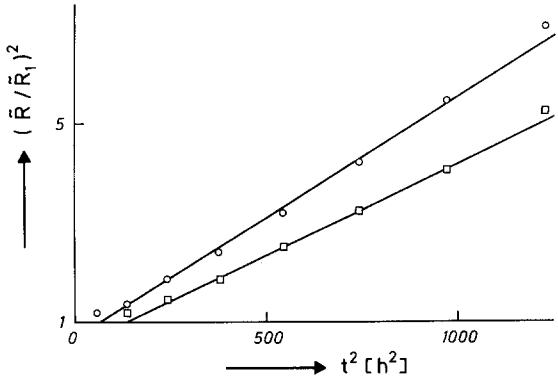

Fig. 11. Plots of the apparent parameters $(\tilde{R}/\tilde{R}_1)^2$ versus the square of the time t of irradiation for unliganded malate synthase ($c = 7.8$ mg/ml) showing the effect of addition of ethanol in the absence of *DTT*. **1** (○): no ethanol; 2 (□): 10 *mM* ethanol

Part II; therein we will also present results from further aggregation experiments and from studies of the X-ray induced inactivation of the enzyme.

Acknowledgements

We wish to express gratitude to Professor Dr. *J. Schurz*, Graz, and to Professor Dr. *R. Jaenicke*, Regensburg, for their interest in the problem. Skilful assistence by Mrs. *G. Durchschlag* in preparing the enzyme is gratefully acknowledged. *H. D.* thanks the Deutsche Forschungsgemeinschaft for support.

References

[1] *D. T. O. Wong* and *S. J. Ajl*, J. Amer. Chem. Soc. **78**, 3230 (1956).
[2] *H. L. Kornberg* and *H. A. Krebs*, Nature (Lond.) **179**, 988 (1957).
[3] *G. H. Dixon*, *H. L. Kornberg*, and *P. Lund*, Biochim. Biophys. Acta **41**, 217 (1960).
[4] *H. Eggerer* and *A. Klette*, Eur. J. Biochem. **1**, 447 (1967).
[5] *H. Durchschlag*, *G. Biedermann*, *G. Durchschlag*, and *H. Eggerer*, Xth Int. Congr. Biochem., Hamburg, Abstr. Nr. 04-6-354 (1976).
[6] *H. Durchschlag*, *K. Goldmann*, *P. Zipper*, and *R. Jaenicke*, Hoppe-Seyler's Z. Physiol. Chem. **357**, 256 (1976).
[7] *H. Durchschlag*, *S. Wenzl*, *G. Durchschlag*, and *R. Jaenicke*, Hoppe-Seyler's Z. Physiol. Chem. **357**, 256 (1976).
[8] *H. Durchschlag*, *K. Goldmann*, *S. Wenzl*, *G. Durchschlag*, and *R. Jaenicke*, FEBS Letters **73**, 247 (1977).
[9] *H. Durchschlag*, *F. Bogner*, *D. Wilhelm*, *R. Jaenicke*, *P. Zipper*, and *F. Mayer*, Hoppe-Seyler's Z. Physiol. Chem. **359**, 1077 (1978).
[10] *P. Zipper* and *H. Durchschlag*, Biochem. Biophys. Res. Commun. **75**, 394 (1977).
[11] *P. Zipper* and *H. Durchschlag*, Eur. J. Biochem. **87**, 85 (1978).
[12] *P. Zipper* and *H. Durchschlag*, Z. Naturforsch. **33 c**, 504 (1978).
[13] *P. Zipper* and *H. Durchschlag*, Acta Crystallogr. **A 31**, S 59 (1975).
[14] *P. Zipper* and *H. Durchschlag*, Rad. Environm. Biophys., in press (1980).
[15] *H. Dertinger* and *H. Jung*, Molekulare Strahlenbiologie. Berlin-Heidelberg-New York: Springer. 1969.
[16] *H. Schüßler*, Biophysik **9**, 315 (1973).
[17] *O. Yamamoto*, in: Advances in Experimental Medicine and Biology, Vol. 86 A (*M. Friedman*, ed.): Protein Crosslinking. Biochemical and Molecular Aspects, pp. 509—547. New York-London: Plenum Press. 1977.
[18] *K. R. Lynn*, in: Advances in Experimental Medicine and Biology, Vol 86 A (*M. Friedman*, ed.): Protein Crosslinking. Biochemical and Molecular Aspects, pp. 557—570. New York-London: Plenum Press. 1977.
[19] *D. A. Armstrong* and *J. D. Buchanan*, Photochem. Photobiol. **28**, 743 (1978).
[20] *P. Zipper* and *H. Durchschlag*, Mh. Chem., in press (1980).
[21] *E. J. Simon* and *D. Shemin*, J. Amer. Chem. Soc. **75**, 2520 (1953).
[22] *G. Biedermann*, Thesis, Universität Regensburg (1972).
[23] *O. Kratky*, Z. Elektrochem. **62**, 66 (1958).
[24] *O. Kratky* and *Z. Skala*, Z. Elektrochem. **62**, 73 (1958).
[25] *P. Zipper*, Acta Phys. Austriaca **30**, 143 (1969).
[26] *O. Kratky*, *I. Pilz*, and *P. J. Schmitz*, J. Colloid Interface Sci. **21**, 24 (1966).

[27] *H. Leopold*, Z. angew. Physik **25**, 81 (1968).
[28] *P. Zipper*, Acta Phys. Austriaca **36**, 27 (1972).
[29] *O. Glatter*, J. Appl. Cryst. **7**, 147 (1974).
[30] *P. Zipper* and *O. Glatter*, Abstr. 4th Int. Conf. on Small-Angle Scattering of X-Rays and Neutrons, Gatlinburg (U.S.A.), p. 49 (1977).
[31] *G. Porod*, Kolloid-Z. **124**, 83 (1951).
[32] *A. Guinier* and *G. Fournet*, Small-Angle Scattering of X-Rays. New York: J. Wiley; London: Chapman & Hall. 1955.
[33] *O. Kratky*, Progr. Biophys. molec. Biol. **13**, 105 (1963).
[34] *O. Kratky* and *I. Pilz*, Quart. Rev. Biophys. **5**, 481 (1972).
[35] *I. Pilz*, *O. Glatter*, and *O. Kratky*, in: Methods in Enzymology, Vol. 61 (*C. H. W. Hirs* and *S. N. Timasheff*, eds.), pp. 148—249. New York-San Francisco-London: Academic Press. 1979.
[36] *O. Kratky*, *G. Porod*, and *Z. Skala*, Acta Phys. Austriaca **13**, 76 (1960).
[37] *P. Zipper* and *H. Durchschlag*, Z. Naturforsch., in press (1980).
[38] *P. Zipper*, *D. Schubert*, and *J. Vogt*, Eur. J. Biochem. **36**, 301 (1973).
[39] *G. Oster*, J. Colloid Sci **2**, 291 (1947).
[40] *H. Schuessler*, Int. J. Radiat. Biol. **27**, 171 (1975).